Cell. Mol. Biol. (ISSN: 1165-158X)

Journal Homepage: www.cellmolbiol.org

Cellular and Molecular Biology

Original Article

Targeting acetate kinase of *Porphyromonas gingivalis*: a computational approach to identifying novel inhibitors for endodontic infection treatment

Nezar Boreak[1*], Shatha Ahmad Jafari[1], Huriyyah Meshal Alotaibi[2], Thekra Saud Abdullah Abbas[1], Abdullah Mohammed Bokar[1], Hajer Bader Muaddi[1], Reem Alshammakhy[1], Ghadeer Ahmed Almughallis[1], Musab Hassan Abdullah Judayba[1], Essa Mohammed Hakami[1]

[1] *Department of Restorative Dental Sciences, College of Dentistry, Jazan University, Jazan 45142, Saudi Arabia*
[2] *College of Dental Medicine, Umm al-Qura University, 21955, Kingdom of Saudi Arabia*

Article Info

Article history:

Received: September 11, 2024
Accepted: December 19, 2024
Published: February 28, 2025

Use your device to scan and read the article online

Abstract

This study explores a novel approach to treating endodontic infections by targeting the acetate kinase (Ack) enzyme of *Porphyromonas gingivalis*, a key pathogen in these infections. Using computational methods, we developed an apo receptor-based E-pharmacophore model of *P. gingivalis* Ack and screened the ZINC Lead-Like database containing over 1.8 million compounds. High-throughput virtual screening and molecular dynamics simulations identified ZINC001306857494 as a promising lead compound, demonstrating stable binding to the Ack active site with a binding free energy of -41.66 kcal/mol. The compound forms multiple hydrogen bonds with highly conserved residues, including Leu119, His180, and Arg241. Molecular dynamics simulations over 250 ns confirmed the stability of the protein-ligand complex, with sustained interactions throughout the simulation period. This study presents a potential new scaffold for developing Ack inhibitors, offering a promising avenue for treating endodontic infections caused by *P. gingivalis*.

Keywords: Endodontic infections, Acetate kinase, High-throughput virtual screening, Molecular dynamics simulations, *Porphyromonas gingivalis*.

1. Introduction

Endodontic Infections are inflammatory diseases majorly caused due to microbial invasion into the oral root canal system, which results in a significant impact on dental health due to their diverse and complex etiology leading to severe complications [1, 2]. Endodontic infection can be classified into two categories (i) Primary and (ii) Secondary infection with primary infection being caused when tooth pulp is infected and colonized by oral microbes, whereas secondary is mostly caused due to persistent root canal infection following endodontic treatment or extension to introduction or retention during the initial treatment of primary [3]. Among the disparate microflora responsible for these infections *Porphyromonas gingivalis*, a Gram-Negative anaerobe commonly associated with periodontal infections, is known to play a crucial role in aggravating the endodontic infection [4].

The *P. gingivalis*, unable to ferment carbohydrates, relies primarily on amino acid catabolism for energy production. The key pathway for ATP generation involves phosphotransacetylase (Pta) and acetate kinase (Ack). Pta converts acetyl-CoA to acetyl phosphate (AcP), which Ack then converts to acetate, generating ATP through substrate-level phosphorylation. This Pta-Ack pathway is crucial for *P. gingivalis* energy metabolism, as evidenced by the co-transcription of pta and ack genes as an operon and the essential nature of Ack for bacterial survival. *P. gingivalis* also demonstrates metabolic flexibility, preferentially metabolizing glutamate/glutamine and aspartate/asparagine, with the latter associated with increased acetate production and ATP formation. Additionally, it can utilize non-proteinaceous substrates like pyruvate and lactate, especially in the presence of human serum. This metabolic adaptability likely contributes to *P. gingivalis*' pathogenicity and persistence in host tissues, underscoring the importance of understanding its energy production mechanisms for potential therapeutic interventions [5, 6]. Therefore, targeting Acetate Kinase (Ack) of *P. gingivalis* could be promising approach for treating endodontic infection and potentially reduce the risk of associated systemic conditions as Ack plays a crucial role in its survival and energy metabolism. By inhibiting Ack, we could potentially disrupt *P. gingivalis* ability to generate energy, thereby limiting its growth and virulence. This approach is

* Corresponding author.
E-mail address: nboraak@jazanu.edu.sa (Nezar Boreak).
Doi: http://dx.doi.org/10.14715/cmb/2025.71.2.15

particularly valuable because both pta and ack genes have been shown to be essential for *P. gingivalis*, making Ack an attractive drug target. Currently, there are no commercially available treatments specifically targeting acetate kinase in *P. gingivalis*. However, research is ongoing to identify potential inhibitors. In this article, we tried to explore the potential for looking for novel inhibitors using Pharmacophore hypothesis and identify the potential scaffold, which could lead to the development of new therapeutic agents.

2. Materials and Methods

2.1. Binding site analysis and protein structure preparation

The Crystal structure of *P. gingivalis* Acetate Kinase was retrieved from Protein Data Bank PDB ID: 6IOY (https://www.rcsb.org/structure/6IOY). The Structure was prepared using Schrodinger's Protein Preparation Wizard. Structural inconsistencies and Hydrogen bonds were optimized, Bond orders and formal charges were added for hetero groups and hydrogen atoms were added to all atoms in the system. The protein molecule was optimized at neutral pH. Structure minimization was performed using OPLS4 force field by converging heavy atoms to RMSD of 0.3 Å. The active site was predicted using SiteMap module of Schrodinger and ranked on the basis of SiteScore and Drugability Score.

2.2. Apo receptor-based E-pharmacophore model generation

The receptor-based E-Pharmacophore model was generated using the predicted active site residues of Acetate Kinase. Apo E-pharmacophore was generated by optimizing the energies onto the atoms. Phase provides a standard set of six pharmacophore features, hydrogen bond acceptor (A), hydrogen bond donor (D), hydrophobic group (H), negatively ionizable region (N), positively ionizable region (P) and aromatic ring (R). Pharmacophore sites were generated from the Receptor Cavity with Phase [7].

2.3. Database screening

The generated E-pharmacophores were taken for Shape-based similarity screening using Schrodinger's Phase Suite. The Screening was carried out using flexible search against Zinc Lead-Like database containing >18,00,000 Lead-Like molecules. Conformers were generated to all tautomers which matched 4 out of 7 pharmacophore features with distance matching tolerance of 3.0 [8]. Receptor-based excluded volumes were integrated to refine the screening process, which helps in reducing false positives. Hits obtained from shape screening based on the e-pharmacophore models were exported as a library.

2.4. High throughput virtual screening

The hypothesis-based screen library was used for molecular docking using High Throughput Virtual Screen to propose novel inhibitors for Acetate Kinase using Glide. A receptor Grid of 10 x 10 x 10 Å was generated on binding site residues of Acetate Kinase. Ligands were prepared and chemical correctness was achieved to expand protonation, stereochemical, ionization variations, energy minimization and tautomeric states at pH 7.0±2.0 units using LigPrep and Epik [9]. The prepared library of Acetate Kinase Inhibitor was than docked into the binding site

2.5. Molecular docking simulation

Desmond Module was used to execute the molecular dynamics calculation [10] for assessing the stability of Acetate kinase-lead docking complex. The docked complex was immersed in the orthorhombic box of the simple point charge (SPC) solvent model. During the simulation process, the buffer box size calculation was employed, and the distance (Å) and angle (°) used were a = 10, b = 10, c = 10, and α = 90°, β = 90°, γ = 90°, respectively. The solvated system was neutralized with counter ions at a physiological NaCl salt concentration of 0.15 M. The OPLS4 force field was used throughout the system preparation steps of the MD simulation [11]. A total of 1000 frames were produced throughout the MD simulation procedure, with the trajectory's recording interval 250 ps. Using the NPT assembly class, the simulation was run for 250 ns at 300 K in temperature and 1.013 bar of atmospheric pressure.

2.6. Statistical analysis

We employed various statistical analyses to evaluate the binding affinities and stability of the lead compounds targeting acetate kinase (Ack) from Porphyromonas gingivalis. The docking scores were analyzed using one-way ANOVA to determine significant differences among the top compounds, with a significance threshold set at $p<0.05p<0.05$. Additionally, Root Mean Square Deviation (RMSD) values from molecular dynamics simulations were calculated to assess the stability of the protein-ligand complexes over a 250 ns period. The number of hydrogen bonds formed between the compounds and Ack was quantified, and a Kruskal-Wallis test was applied to analyze differences in interaction strength. Finally, Pearson correlation coefficients were used to evaluate the relationship between conservation scores of interacting residues and binding affinities, providing a comprehensive statistical framework for our findings.

3. Results

Structure-based pharmacophore modelling is performed on atomistic models of two different types (i) The Protein-Ligand Complex and (ii) Apo-Protein (macromolecules with no known ligands for binding site). Apo 3D pharmacophore modeling is useful in necessitating de-novo approaches to pharmacophore placement within the active site, offering the potential for scaffold hopping and identification by utilizing the arrangement of abstract features that are not tied to any specific ligand structure [12]. Here, we employed Apo Feature-based 3D pharmacophore modeling for the identification of potential inhibitors of Acetate Kinase of *P. gingivalis.* In feature-based methods, fragments are docked into the apo site using the Glide XP docking program [12, 13], and the energetically favorable fragments posed are then selected to construct pharmacophore hypothesis using Phase [14].

3.1. Generation of the E-pharmacophore model

An Energy-optimized pharmacophore hypothesis was developed using "Develop a Pharmacophore from Receptor Cavity" option in the phase module using SiteMap generated Site (Figure 1A and Table 1). The hypothesis was set at a maximum feature-feature distance of 2.5 Å. Seven Pharmacophore sites were identified and the final hypothesis consisted of two aromatic rings (R19 and R20),

three negatively ionizable regions (N13, N14 and N15), one hydrogen bond donor(D9) and one aromatic ring (A4) as shown in Figure 1B.

Due to the lack of any known inhibitors of Acetate Kinase, the developed pharmacophore model could not be validated. However, considering the importance and need of searching for potential scaffold and inhibitor, we continued the study and used the model for further Screening of Zinc Lead-Like molecules.

3.2. PHASE screen

Phase screen was carried out on receptor-based pharmacophore to screen for the possible Acetate Kinase Inhibitor of *P. gingivalis*. The Screen was carried out on 4 out of 7 hypotheses, allowing only compounds that matched 4 out of 7 pharmacophoric sites. The screen identified total of 5401 molecules out of 18,00,000 screened molecules.

3.3. High throughput virtual screen

High throughput Virtual Screening was performed on the screen-identified molecule using Schrodinger Virtual Screen Workflow. The Screen was performed using three steps. (i) Docking with Glide HTVS, (ii) Dock with Glide SP and (iii) Dock with Glide XP. The Docking was performed Flexibly in all the steps. During the initial two steps, only 1% of the best molecules were kept while retaining the only best Scoring state (Table 1). In the third step, we just kept the top 3 of the best compounds for further analysis due to computational restrictions (Table 2). These Compounds were further processed with Prime MM-GBSA to further refine and Calculate the Free Binding Energy.

At the Active site of ZINC001306857494 was found to bind with acetate kinase with Binding Free energy of -41.66Kcal/mol. It was found to be stabilized by 6 H-bond interactions. The amino acid Leu 119 was found to form two hydrogen bonds, while Arg 241 formed three hydrogen bonds, and His 180 was found to form a single hydrogen bond interaction (Figure 2B). The Second Hit ZINC000584898641 was found to bind at the active site

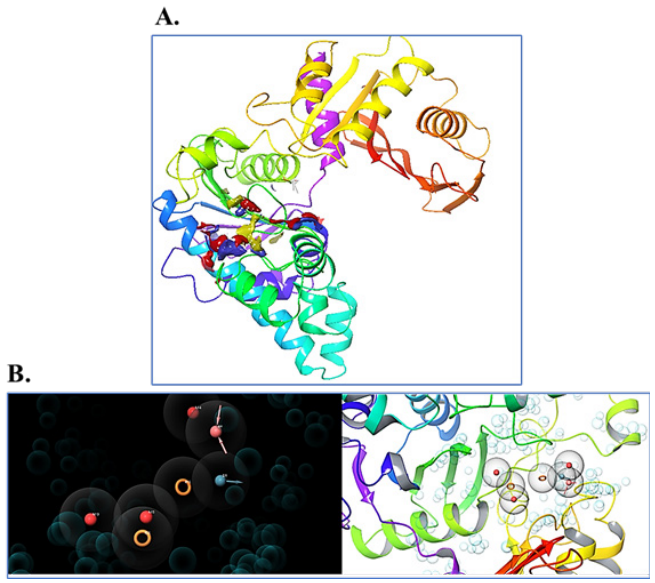

Fig. 1. (A) Predicated active site of AckPg (B) Developed Apo-Pharamcophore-based hypothesis at the binding site of AckPg.

Table 2. The Top 3 Screened lead like molecules through HTVS Screening.

Molecule	Docking Score	dG Bind (Kcal/mol)
ZINC001306857494	-7.334	-41.66
ZINC001274926025	-7.227	-40.16
ZINC000584898641	-7.107	-41.44

Table 1. Top lead-like molecules from HTVS Screening.

Active Site	DScore	SiteScore	Volume	Residues
Site 1	0.906	0.899	262.052	162,164,174,229,230,231,232,233,234,242,243,244,245,247,250,265,268,269, 501,693,716

Title	docking_score	Title	docking_score	Title	docking_score
ZINC001147693083	-7.12984	ZINC000677868386	-6.56726	ZINC000011693088	-6.28338
ZINC001306857494	-7.08364	ZINC001275545409	-6.53424	ZINC001276559095	-6.28292
ZINC001212665287	-7.03932	ZINC001274926025	-6.49244	ZINC000091486755	-6.25304
ZINC000021704371	-6.82549	ZINC001270176986	-6.47804	ZINC001365237288	-6.2363
ZINC001176265302	-6.80745	ZINC001168921162	-6.46168	ZINC001364165635	-6.22916
ZINC001168919875	-6.79909	ZINC001167358939	-6.43273	ZINC001165685926	-6.19703
ZINC000820385512	-6.79156	ZINC001275265738	-6.43187	ZINC001455983478	-6.19156
ZINC001168924431	-6.78293	ZINC001269702772	-6.41429	ZINC001275820411	-6.18949
ZINC000566941774	-6.78054	ZINC001219741917	-6.3989	ZINC001245927008	-6.18606
ZINC001152382881	-6.70345	ZINC001278238954	-6.38131	ZINC000002150471	-6.18598
ZINC001219741765	-6.66529	ZINC001320624126	-6.37262	ZINC001147689514	-6.17766
ZINC000354178254	-6.60908	ZINC001195541723	-6.34532	ZINC000000712182	-6.16846
ZINC001274849975	-6.60241	ZINC001196209405	-6.34034	ZINC001301192276	-6.16811
ZINC001270138920	-6.6019	ZINC000584898641	-6.33266	ZINC001261759057	-6.1599
ZINC001269346922	-6.59106	ZINC001163017803	-6.322		
ZINC001474282880	-6.58825	ZINC001434449974	-6.32124		
ZINC001336896811	-6.57902	ZINC001157934379	-6.30037		

with binding free energy of -41.44 Kcal/mol. The molecule was found to form 3 H-bond interactions. Amino acid residue Lue 119, Arg241 and His 180 were found to form single H-bond interaction. Similarly, ZINC001274926025 was found to be bound with binding Free energy of -40.16Kcal/mol, in addition to H bond Interaction with Leu119. The compound formed an H bond interaction with His123 and Arg 91.

We further looked into the interaction of these compounds using the ConSurf analysis to understand whether the docking interactions are aligned with evolutionarily conserved regions (Figure 2A). It was observed that all the interacting amino acid residues Leu 119, His180, Arg24, His 123, and Arg91 are highly conserved across the evolution among all the Acetate Kinase proteins (Figure 2C). Thus, this suggests that the binding of these compounds occurs within structurally and functionally important regions.

3.4. Molecular dynamic simulation

Molecular Dynamics is a crucial tool for studying the interaction between protein-ligand complexes and generation of accurate computer-aided drug design. In the current study, the top 3 poses from virtual screening were subjected to Molecular dynamic simulation of 250ns to understand the stability of protein-ligand complexes and provide keen insights into the binding modes and conformational changes of both ligand and protein.

3.4.1. Analysis of RMSD value of proteins and ligands

The molecular dynamics (MD) simulation results were analyzed using Cα and ligand root mean square deviation (RMSD) values, providing insights into conformational changes of the protein-ligand complexes relative to their initial structures. The protein RMSD trajectories for most complexes exhibited deviations ranging from 1.5 Å to 3.5 Å, rarely exceeding 4 Å3. However, the ZINC001274926025 complex demonstrated a progressive increase in Cα RMSD throughout the simulation, indicating significant instability. For the ZINC001306857494 complex, the Cα RMSD increased during the initial 25 ns before reaching a plateau. A brief fluctuation around 98 ns resulted in an RMSD slightly exceeding 4 Å, after which the protein backbone maintained an average RMSD of approximately 3.5 Å for the remainder of the simulation. The ligand RMSD rapidly increased from 1 Å to 2.5 Å within the first 10 ns, subsequently fluctuating between 2.5 Å and 4 Å throughout the simulation. This behavior suggests a stable protein-ligand complex capable of maintaining molecular interactions (Figure 3A).

In contrast, the ZINC000584898641-protein complex exhibited more complex dynamics. While the Cα RMSD remained below 3.5 Å throughout the simulation, the ligand RMSD displayed substantial fluctuations. Initially stable at around 2 Å for the first 50 ns, the ligand RMSD subsequently increased dramatically, exceeding 4 Å after 50 ns and surpassing 7 Å beyond 75 ns. This significant shift in RMSD values can be attributed to conformational changes of the ligand within the binding site, ultimately resulting in its complete displacement (Figure 3B). These findings highlight that ZINC001306857494 is much more stable compared to its other 2 counterparts and may have the potential to inhibit the acetate kinase of *P. gingivalis*.

3.4.2. Analysis of RMSF

The RMSF analysis was performed to aim at the conformational changes of protein that occurred due to the binding of ligands during simulation, As RMSF of each

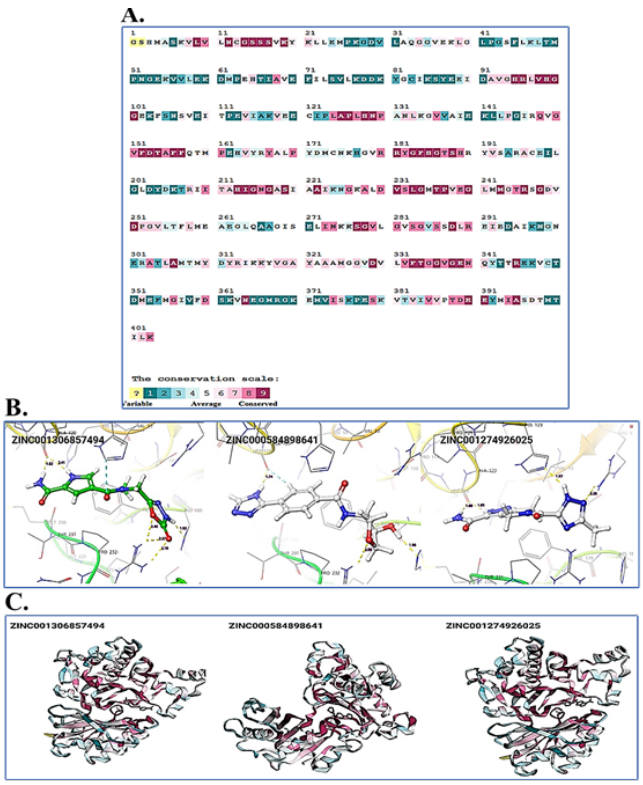

Fig. 2. (A) Consurf analysis of Acetate Kinase of P gingivalis (B) Top 3 Lead molecules binding at the active site of Ackpg (C) Consurf Analysis of top3 lead-like molecules and their interaction with Highly Conserved amino acid residues.

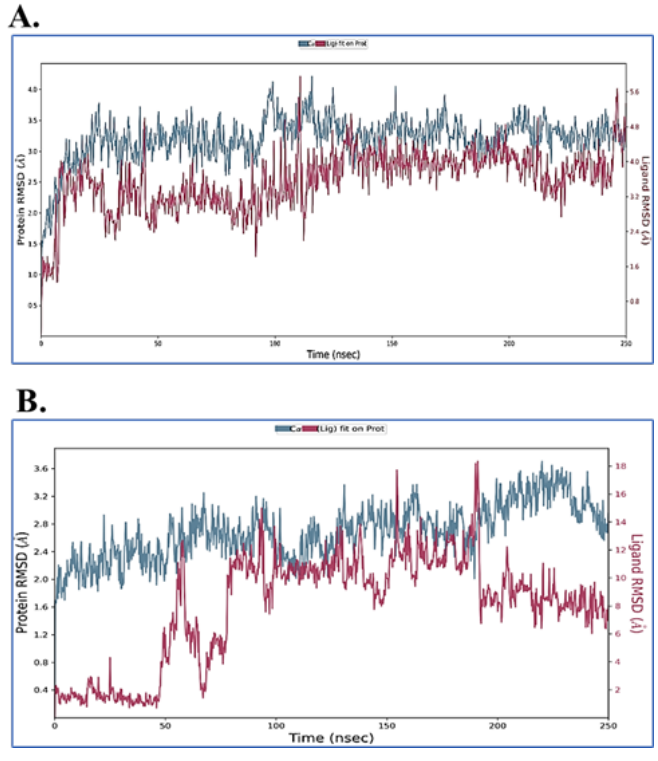

Fig. 3. (A) RMSD analysis of ZINC001306857494.The red shows the fluctuation of Ligand w.r.t the protein. Blue shows RMSD of C-alpha atoms of protein during the simulation. (B) Protein-Ligand RMSD of ZINC000584898641.

system helps in understanding the stability and movement of each residue. A plot with increased fluctuations indicates an unstable connection. Similarly, on the other hand, lower or reduced fluctuation suggests well-structured, stable and less distorted complex regions. The stability of the compounds with Acetate Kinase was confirmed by finding the interacting active site residues and showed no change overtime in the case of ZINC001306857494 (Figure 4A) and ZINC000584898641 (Figure 4B). However, in the case of ZINC001274926025 the RMSF values were found to be quite high suggesting unstable interactions.

3.4.3. Ligand protein contact analysis

The Ligand protein contact analysis during the simulation provides valuable insights into the molecular interaction, interaction strength and key interactors. The Ligand protein contact analysis revealed that only ZINC001306857494 was able to maintain sustainable contacts throughout the simulation while maintaining the contact strength >30% with amino acid resides His123, His180, Leu122 and Ser265. In addition to H bond contacts, pi-pi stacking and pi-cation interaction were also observed with amino acid His123 and Arg 241 respectively (Figure 5A). In contrast, both ZINC000584898641 and ZINC001274926025 were not able to maintain any significant contacts, suggesting ZINC001306857494 as only potential lead (Figure 5B and 5C).

4. Discussion

Considering the role of *P. gingivalis* in endodontic infections, the search for new drugs targeting the pathogen might help in the prevention, treatment and maintenance of oral hygiene. To date, there are only a few studies performed to identify the drugs targeting *P.gingivalis* but none of them were designed to target Acetate Kinase [15, 16]. Kohler et.al in a preliminary computational study screened streptomeDB against the Acetate Kinase. However, in the current study, we attempted to screen a large database of Zinc Database -Lead-like molecules (>1800000) using the Apo pharmacophore hypothesis-based approach. In an attempt to identify a novel molecule or scaffold that can potentially inhibit the Acetate Kinase enzyme.

In this study, the molecules from zinc database were recruited to identify a novel molecule against the active site of AcK. Our analysis suggested that amino acid residues within the active site of *P. gingivalis* are highly conserved and the interaction of most lead molecules with amino acid Leu 119, His180, Arg241, His 123, Arg91. Considering

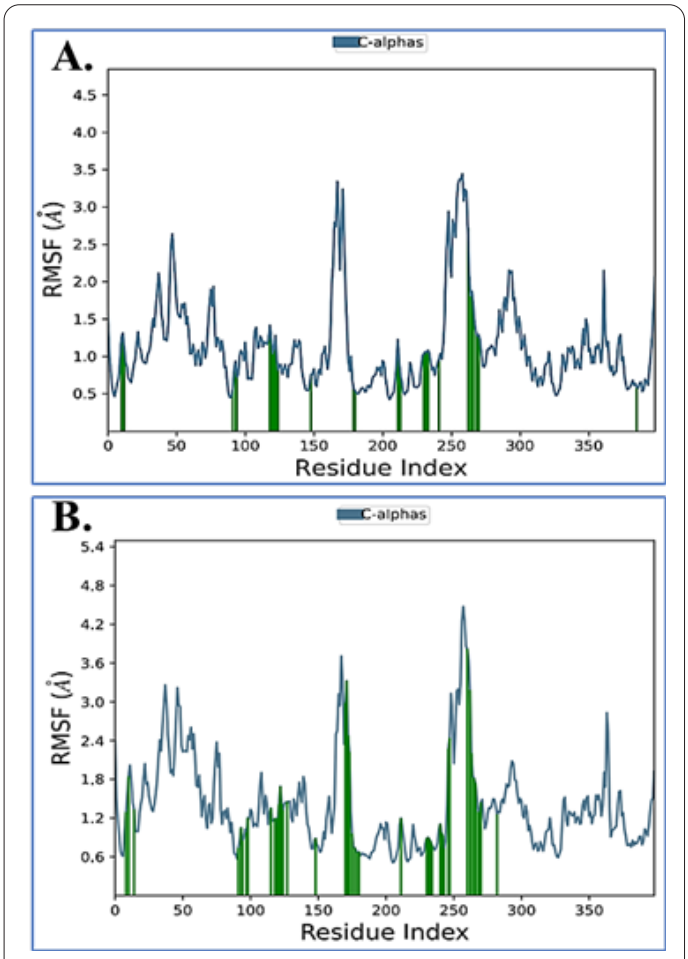

Fig. 4. (A) RMSF analysis of ZINC001306857494.Green lines denote the ligand interacting residues (B) RMSF analysis of ZINC000584898641.

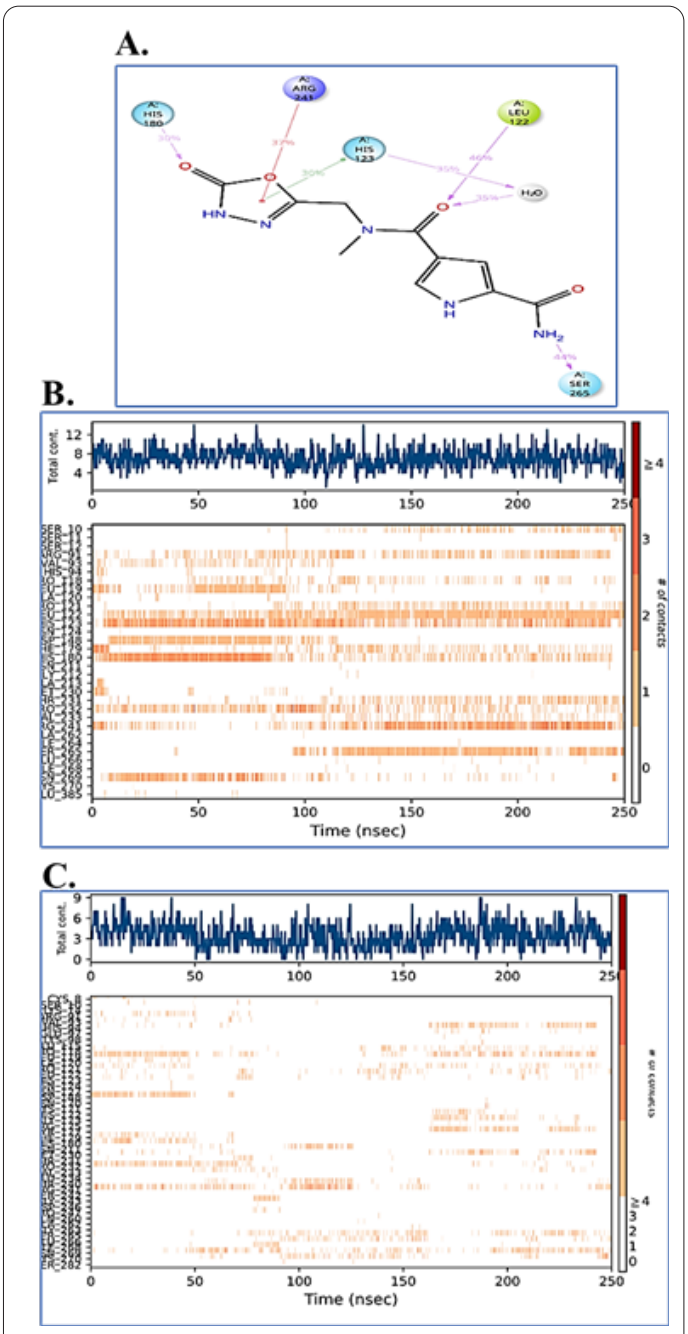

Fig. 5. (A) 2D interaction diagram of ZINC001306857494 showing strength of interaction during the simulation (B) Contact Timeline of ZINC001306857494 (C) Contact Timeline of ZINC000584898641.

their higher extent of conservation these residues can be considered critical for drug designing.

The physiochemical and pharmacodynamic properties were evaluated. The molecule was not found to violate any of the Lipiniskis rule of 5. it is well known that most orally available molecules follow the rule of five [17]. We found that the identified scaffold 1,3,4-oxadiazole, a five-membered, conjugated, planar, and stable heteroaromatic ring containing two nitrogen atoms at the 3 and 4 positions, and an oxygen atom at position 1 is well known for its role in anti-microbial activity and anti-inflammatory activities [18]. Apart from antimicrobial activity, these compounds have been studied for decades due to their promising biological activities such as anti-Covid, anti-fungal, anti-viral, anti-cancer, and anti-diabetic activity [19, 20].

1,3,4-Oxadiazole derivatives have emerged as promising kinase inhibitors, demonstrating significant potential in the treatment of various diseases, particularly cancer and neurodegenerative disorders. 3,4-Oxadiazole derivatives have shown promise as inhibitors of GSK-3β, a kinase implicated in the abnormal hyperphosphorylation of tau protein associated with Alzheimer's disease [21]. Recent computational studies have explored 1,3,4-oxadiazole derivatives as potential inhibitors of VEGFR2, a key target in renal cancer treatment [22], suggesting the 1,3,4-oxadiazole derivatives as promising candidates for the development of novel and effective kinase inhibitors.

The current study is an in-silico analysis, which inherently presents several methodological limitations. While computational approaches provide valuable initial insights into potential drug candidates, they necessitate comprehensive validation through experimental methods. Specifically, wet-lab analyses, including detailed pharmacokinetics and pharmacodynamics assays, are crucial to definitively evaluate the draggability and potential therapeutic efficacy of the proposed compounds.

Our computational study has identified ZINC001306857494 as a potential inhibitor of *P. gingivalis* acetate kinase, a crucial enzyme for the pathogen's survival and energy metabolism. The compound's stability in molecular dynamics simulations and its interactions with highly conserved residues in the Ack active site suggests its potential as a lead for developing novel therapeutics against endodontic infections. The 1,3,4-oxadiazole scaffold of ZINC001306857494 offers a promising starting point for further optimization and drug development. While experimental validation is necessary, this study demonstrates the power of structure-based pharmacophore modeling and virtual screening in identifying new drug candidates for challenging bacterial targets. Future research should focus on in vitro and in vivo studies to confirm the efficacy and safety of this compound, potentially leading to new treatments for endodontic infections and associated systemic conditions.

Institutional review board statement
Not applicable.

Informed consent statement
Not applicable.

Data availability statement
All data are available online. No unpublished data have been used in this paper.

Acknowledgments
The authors gratefully acknowledge the funding of the Deanship of Graduate Studies and Scientific Research, Jazan University, Saudi Arabia, through Project Number: GSSRD-24.

Conflicts of interest
The authors declare no conflicts of interest.

References

1. Boreak N, Alrajab EA, Nahari RA, Najmi LE, Masmali MA, Ghawi AA, Al Moaleem MM, Alhazmi MY, Maqbul AA (2024) Unveiling Therapeutic Potential: Targeting Fusobacterium nucleatum's Lipopolysaccharide Biosynthesis for Endodontic Infections—An In Silico Screening Study. Int J Mol Sci 25 (8): 4239. doi: https://doi.org/10.3390/ijms25084239
2. Rezaie-Kahkhaie L, Saravani K, Rezaie-Keikhaie K, Azimi-Khatibani SE, Daman-Sooz AH, Afshari M, kamali A (2021) Prevalence of hepatitis B in HIV-positive patients in Zabol. Cell Mol Biomed Rep 1 (3): 105-112. doi: Https://doi.org/10.55705/cmbr.2021.356667.1058
3. Saygun I, Nizam N, Keskiner I, Bal V, Kubar A, Açıkel C, Serdar M, Slots J (2011) Salivary infectious agents and periodontal disease status. J Periodontal Res 46 (2): 235-239. doi: https://doi.org/10.1111/j.1600-0765.2010.01335.x
4. Tomazinho LF, Avila-Campos MJ (2007) Detection of *Porphyromonas gingivalis*, *Porphyromonas endodontalis*, *Prevotella intermedia*, and *Prevotella nigrescens* in chronic endodontic infection. Oral Surg Oral Med Oral Pathol Oral Radiol Endod 103 (2): 285-288. doi: https://doi.org/10.1016/j.tripleo.2006.05.010
5. Takahashi N, Sato T, Yamada T (2000) Metabolic pathways for cytotoxic end product formation from glutamate-and aspartate-containing peptides by Porphyromonas gingivalis. J Bacteriol 182 (17): 4704-4710. doi: https://doi.org/10.1128/jb.182.17.4704-4710.2000
6. Takahashi N, Sato T (2001) Preferential utilization of dipeptides by Porphyromonas gingivalis. J Dent Res 80 (5): 1425-1429. doi: https://doi.org/10.1177/00220345010800050801
7. Pradeep N, Munikumar M, Swargam S, Hema K, Sudheer Kumar K, Umamaheswari A (2015) 197 Combination of e-pharmacophore modeling, multiple docking strategies and molecular dynamic simulations to discover of novel antagonists of BACE1. J Biomol Struct Dyn 33 (sup1): 129-130. doi: https://doi.org/10.1080/07391102.2015.1032834
8. Venkatraman V, Pérez-Nueno VI, Mavridis L, Ritchie DW (2010) Comprehensive comparison of ligand-based virtual screening tools against the DUD data set reveals limitations of current 3D methods. J Chem Inf Model 50 (12): 2079-2093. doi: https://doi.org/10.1021/ci100263p
9. Greenwood JR, Calkins D, Sullivan AP, Shelley JC (2010) Towards the comprehensive, rapid, and accurate prediction of the favorable tautomeric states of drug-like molecules in aqueous solution. J Comput Aided Mol Des 24 (6): 591-604. doi: https://doi.org/10.1007/s10822-010-9349-1
10. Maragakis P, Lindorff-Larsen K, Eastwood MP, Dror RO, Klepeis JL, Arkin IT, Jensen MØ, Xu H, Trbovic N, Friesner RA (2008) Microsecond molecular dynamics simulation shows effect of slow loop dynamics on backbone amide order parameters of proteins. J Phys Chem B 112 (19): 6155-6158. doi: https://doi.org/10.1021/jp077018h
11. Lu C, Wu C, Ghoreishi D, Chen W, Wang L, Damm W, Ross GA, Dahlgren MK, Russell E, Von Bargen CD (2021) OPLS4: Improving force field accuracy on challenging regimes of chemical

space. J Chem Theory Comput 17 (7): 4291-4300. doi: https://doi.org/10.1021/acs.jctc.1c00302

12. Schaller D, Šribar D, Noonan T, Deng L, Nguyen TN, Pach S, Machalz D, Bermudez M, Wolber G (2020) Next generation 3D pharmacophore modeling. Wiley Interdiscip Rev Comput Mol Sci 10 (4): e1468. doi: https://doi.org/10.1002/wcms.1468
13. Friesner RA, Murphy RB, Repasky MP, Frye LL, Greenwood JR, Halgren TA, Sanschagrin PC, Mainz DT (2006) Extra precision glide: Docking and scoring incorporating a model of hydrophobic enclosure for protein− ligand complexes. J Med Chem 49 (21): 6177-6196. doi: https://doi.org/10.1021/jm051256o
14. Dixon SL, Smondyrev AM, Knoll EH, Rao SN, Shaw DE, Friesner RA (2006) PHASE: a new engine for pharmacophore perception, 3D QSAR model development, and 3D database screening: 1. Methodology and preliminary results. J Comput Aided Mol Des 20: 647-671. doi: https://doi.org/10.1007/s10822-006-9087-6
15. Rocha-Roa C, Cossio-Pérez R, Molina D, Patiño J, Cardona N (2018) In silico study of *Moxifloxacin derivatives* with possible antibacterial activity against a resistant form of DNA gyrase from *Porphyromonas gingivalis*. Arch Oral Biol 95: 30-39. doi: https://doi.org/10.1016/j.archoralbio.2018.07.015
16. Ma H, Stone VN, Wang H, Kellogg GE, Xu P, Zhang Y (2017) Diaminopimelic acid (DAP) analogs bearing isoxazoline moiety as selective inhibitors against meso-diaminopimelate dehydrogenase (m-Ddh) from *Porphyromonas gingivalis*. Bioorg Med Chem Lett 27 (16): 3840-3844. doi: https://doi.org/10.1016/j.bmcl.2017.06.056
17. Lipinski CA, Lombardo F, Dominy BW, Feeney PJ (2012) Experimental and computational approaches to estimate solubility and permeability in drug discovery and development settings. Adv Drug Deliv Rev 64: 4-17. doi: https://doi.org/10.1016/j.addr.2012.09.019
18. Luczynski M, Kudelko A (2022) Synthesis and biological activity of 1, 3, 4-oxadiazoles used in medicine and agriculture. Appl Sci 12 (8): 3756. doi: https://doi.org/10.3390/app12083756
19. Rabie AM (2021) Two antioxidant 2, 5-disubstituted-1, 3, 4-oxadiazoles (CoViTris2020 and ChloViD2020): successful repurposing against COVID-19 as the first potent multitarget anti-SARS-CoV-2 drugs. New J Chem 45 (2): 761-771. doi: https://doi.org/10.1039/D0NJ03708G
20. Stecoza CE, Nitulescu GM, Draghici C, Caproiu MT, Olaru OT, Bostan M, Mihaila M (2021) Synthesis and anticancer evaluation of new 1, 3, 4-oxadiazole derivatives. Pharmaceuticals 14 (5): 438. doi: https://doi.org/10.3390/ph14050438
21. Saitoh M, Kunitomo J, Kimura E, Hayase Y, Kobayashi H, Uchiyama N, Kawamoto T, Tanaka T, Mol CD, Dougan DR, Textor GS, Snell GP, Itoh F (2009) Design, synthesis and structure–activity relationships of 1,3,4-oxadiazole derivatives as novel inhibitors of glycogen synthase kinase-3β. Bioorg Med Chem Lett 17 (5): 2017-2029. doi: https://doi.org/10.1016/j.bmc.2009.01.019
22. Bilal MS, Ejaz SA, Zargar S, Akhtar N, Wani TA, Riaz N, Aborode AT, Siddique F, Altwaijry N, Alkahtani HM (2022) Computational investigation of 1, 3, 4 oxadiazole derivatives as lead inhibitors of VEGFR 2 in comparison with EGFR: Density functional theory, molecular docking and molecular dynamics simulation studies. Biomolecules 12 (11): 1612. doi: https://doi.org/10.3390/biom12111612